CALIBRATION OF A MOTT POLARIMETER

Valeria Ramírez, C. Hernández-García, J. Grames, R. Suleiman, P. Adderley, G. Palacios-Serrano*

Thomas Jefferson National Accelerator Facility, VA, USA
*Universidad Autónoma del Estado de Hidalgo (Academic Area of Physics and Mathematics), Hgo, Mx

ABSTRACT

The main accelerator of Jefferson Lab uses a Mott Polarimeter to measure the polarization of the electron beam that is going to be used in the CEBAF experiments. The polarimeter is located in the first parts of the beam line, after the beam leaves the electron gun and has not yet accelerated to very high velocities; the use of the polarimeter gives us certainty of the polarization that will be used in the experimental halls. The purpose of the project is to calibrate the Mott polarimeter to ensure its function correctly by calculating the polarization for different values of asymmetry. To accomplish this, first, the polarimeter is assembled with its corresponding elements: vacuum chamber, target ladder, and detectors. To calibrate it, the beam is used to measure the number of electrons that are scattered at different angles when they hit a target foil in the polarimeter. This process is repeated for four target foils of different thicknesses so that the asymmetry and polarization for each one of them can be found.

With the experiment, it is expected to see a decreased value of asymmetry for thicker target foils and an increased value when thinner target foils are used. It is possible to find a graphic that describes the behavior and do an interpolation to obtain the value of the Sherman functions for a thickness of almost zero; this value should be the largest of all and will represent the polarization when we have the electron beam in vacuum. When using the Sherman functions, the polarization of the electron beam can be found. The Mott polarimeter in the main accelerator is used to ensure that the experiments and analyses at the experimental halls in Jefferson Lab have a correct polarization.

1. INTRODUCTION

1.1. Mott scattering

Mott measured the scattering of high energy electrons from massive nuclei (see Fig. 1), in the rest frame of the electron it experiences a magnetic field so that there is an interaction between this field and the magnetic moment, this so-called spin-orbit interaction leads to a term to be added in the potential [2], so the scattering cross section is modified as follows.

$$\sigma(\theta) = \sigma_0(1 + \vec{P} \cdot \hat{n}S) \tag{1}$$

Where $\vec{P}$ is the polarization, S are the so called Sherman functions, σ_0 is the unpolarized cross section defined as

$$\sigma_0 = \left(\frac{Ze^2}{2mc^2}\right)^2 \frac{(1-\beta^2)(1-\beta^2 sin^2(\theta/2))}{\beta^4 sin^4(\theta/2)}$$

and $\hat{n}$ is an unitary vector perpendicular to the plane of scattering, defined by

$$\hat{n} = \frac{\vec{k}\times\vec{k\prime}}{\|\vec{k}\times\vec{k\prime}\|}$$

where $\vec{k}$ is the incident direction of the electron and $\vec{k\prime}$ is the dispersion direction of the electron.

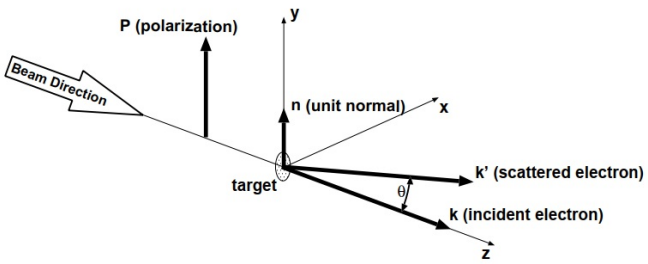

Fig. 1: Diagram of the physics of Mott scattering, where θ is the scattering angle. Figure courtesy of Joe Grames [1].

1.2. The basic equations

The equation (1) depends on the result of the scalar product between $\vec{P}$ and $\hat{n}$, since they are in the same direction, there are only two options:

- Electron with spin down $\otimes$,

$$\sigma_{dn}(\theta) = \sigma_0(1 - PS)$$

- Electron with spin up $\odot$,

$$\sigma_{up}(\theta) = \sigma_0(1 + PS)$$

On the other hand, it is possible to measure the number of electrons scattered an angle θ to the right (N^r) or to the left (N^l) and see that

$$N^r \propto (1 + PS)$$
$$N^l \propto (1 - PS)$$

So the **asymmetry** can be defined as:

$$\boxed{\epsilon = \frac{N^r - N^l}{N^r + N^l}} \tag{2}$$

And in terms of the **polarization**:

$$\boxed{\epsilon = PS} \tag{3}$$

Equations (2) and (3) can be used when the helicity of the electrons has no change, so that N^r and N^l are the number of electrons with either positive or negative helicity but they do not combine with each other.
If its wanted to take into account both helicities, it is needed to define:

$$r = \sqrt{\frac{(N^l_+)(N^r_-)}{(N^l_-)(N^r_+)}} \tag{4}$$

So that:

$$\boxed{\epsilon = \frac{1 - r}{1 + r}} \tag{5}$$

1.3. The Sherman functions

In an experiment, the number of electrons that hit the target in a certain time can be measured, this is called the **rate**:

$$R(\theta) = N/T = \sigma(\theta) L \rho (I/e^-) \tag{6}$$

Where $\sigma(\theta)$ is the cross-section, L is the thickness of the target, ρ is the target density and (I/e^-) is the beam current.

So far, the scattering of an electron from a single atom has been described (Eq. (3) or (5)), however, in a real experiment the target foil contains a lot of atoms since it has a considerable area and thickness, this leads to possible multiple scatterings, when this happens the value of the total scattering is diluted. As it can be seen in the equation (6), if $\sigma(\theta)$ decreases, the number of electrons N decreases too, so that the asymmetry gets reduced when we have a target foil with a lot of atoms (more area/thickness).

2. OUR MOTT SCATTERING POLARIMETER

2.1. Description

Our Mott polarimeter consists in a vacuum chamber (see Fig. 2) where a target ladder that contains 6 holes is mounted (see Fig. 3), one of the holes is left empty, another one is used for the viewer disk and the remaining four contain golden foils of different thicknesses (40 nm, 60 nm, 70 nm and 80 nm), this ladder can go up and down so that a target of a different thickness can be used each time the experiment is performed (see Fig. 4).

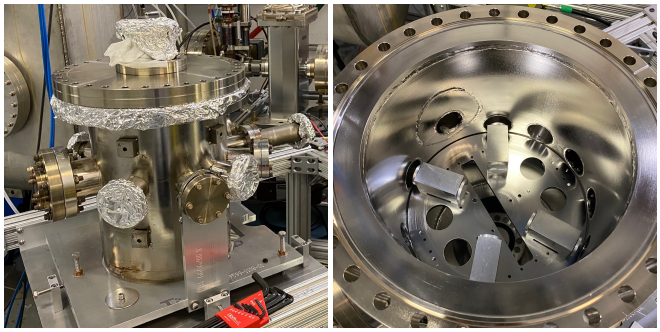

(a) Outside of the vacuum chamber (b) Inside of the vacuum chamber

Fig. 2: Vacuum chamber used for the Mott polarimeter without detectors and target ladder.

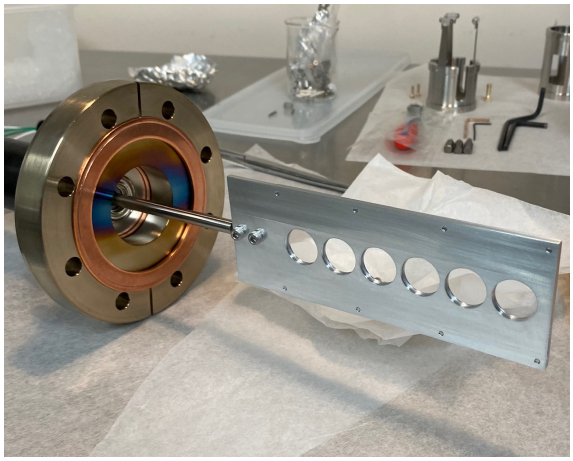

Fig. 3: Unmounted target ladder without golden foils and viewer.

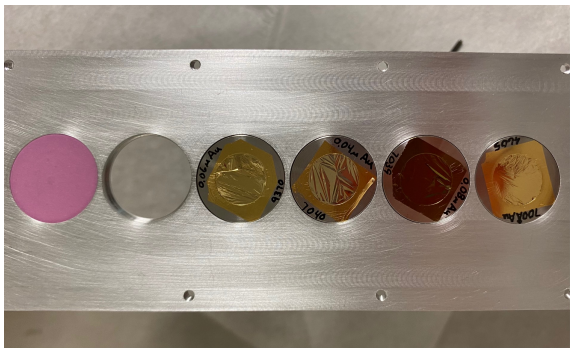

Fig. 4: Target ladder. The pink disk at the left is the viewer disk, the second hole is left empty and the next four disks have the golden foils of thicknesses 60 nm, 40 nm, 80 nm and 70 nm respectively.

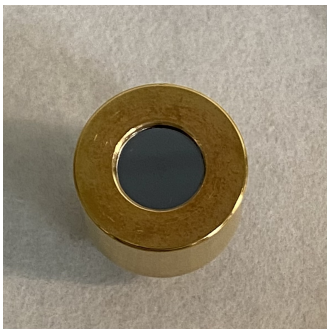

(a) Top view of the detector previous to be mounted and connected.

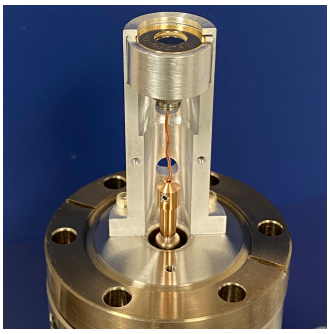

(b) Side view of the detector, connected and assembled.

Fig. 5: One of the two detectors used in the Mott polarimeter previous to be mounted in the vacuum chamber.

Fig. 6: Beam dump used in the polarimeter.

Two detectors are mounted in the internal walls of the vacuum chamber, just as the one that can be seen in figure 5, they measure the electron scattering an angle of 120°.
Finally, there is a beam dump connected to the last part of polarimeter, i.e. to the vacuum chamber, where the electrons that were not scattered can be deposited, on the inside its shaped as a cone so that the energy of the beam can be absorbed. See Fig. 6.

We can observe in Fig. 7 how it looks when everything is mounted and assembled.

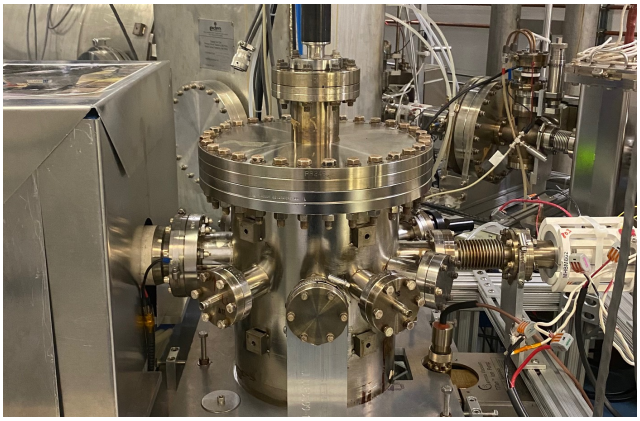

Fig. 7: Mott polarimeter fully mounted and assembled.

2.2. Data acquisition and analysis

Once everything is mounted, it is required to connect the detectors to the data acquisition system (see Fig. 8) using the preamplifiers, we need one preamplifier per detector with its corresponding Test, Power and T-out cables.

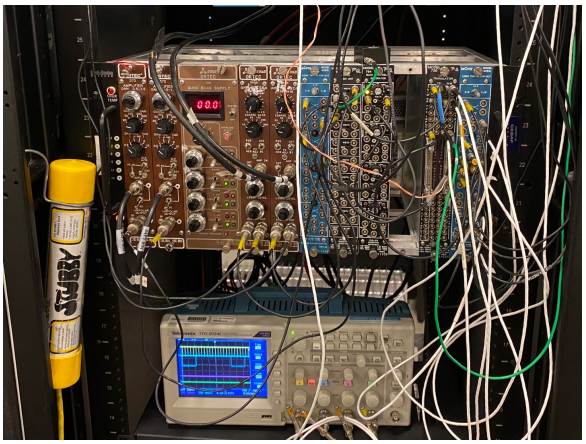

Fig. 8: Data acquisition system.

When the cabling is done, the focus will be on six main channels that represent the following:

- Value of the pulse for the left and right detector for each electron (CH1, CH2): It shows how the energy of each electron changes over time.
- Logical sign for the timing in the left and right detector (CH3, CH4): Measures when to stop taking data.
- Helicity (CH13): It is a digital sign where the high/low values indicate the type of helicity for each electron.
- T-Settle: Indicates how the Pockels cell change and shows the electrons that have discrepancy compared with the rest of the data and should be ignored.

By using this, a program may be written to organize the data coming into the channels and obtain the asymmetry.

2.2.1. Organization of the data

Using the CH1 or CH2 it is possible to sum over all the samples for each e^- to obtain its energy. Then, the value of the helicity showed in CH13 is reassigned to 0 or 1 for the case of negative/positive helicity. Finally, with the T-Settle the unwanted values are left out by assigning them the value of 0.

Once this is done, histograms that show the energy vs the number of electrons can be generated, in this case it is interesting to consider:

- Histograms of electrons whose energy is measured by the **left detector**.

- Histograms of electrons whose energy is measured by the **right detector**.
- Histograms of electrons with **positive helicity** whose energy is measured by the **left detector**.
- Histograms of electrons with **negative helicity** whose energy is measured by the **left detector**.
- Histograms of electrons with **positive helicity** whose energy is measured by the **right detector**.
- Histograms of electrons with **negative helicity** whose energy is measured by the **right detector**.

2.2.2. *Measuring asymmetry*

We want to measure the number of electrons that reach the detectors with clean energy, i.e. that do not lose energy along the way. The highest peak of the histogram will be taken and, by making a Gaussian fit, the electrons between -0.5σ and 2σ of the fit are selected, so that the ones with higher energies are taken.
With these values it is possible to measure the asymmetry as it is stated in the equation (5). The process has to be repeated for all the golden foils with different thicknesses.

3. THE EXPERIMENT

3.1. The beamline

The beamline of our experiment consists in three main elements: an electron gun, the Wien filter and the Mott polarimeter.

3.1.1. *Electron gun*

We will start our experiment by using a longitudinal polarized beam produced by an electron source, i.e. a gun of 180 kV. See Fig. 9.
We obtain this polarization of the electron beam by shooting a photoemission GaAs cathode that is inside of the gun with an external laser that creates a train of optical pulses that are circularly polarized [3, 5].

Its important to notice that the polarization of the electron beam depends on the polarization of the optical beam (laser) in two ways:

- The degrees of polarization depend on each other.
- The helicity of the electron beam polarization depends on the helicity of the photons of the optical beam.

To measure the beam polarization we need to measure the scattering rates between the two helicity states of the electron beam, we can perform this measurement by using Pockels cells.

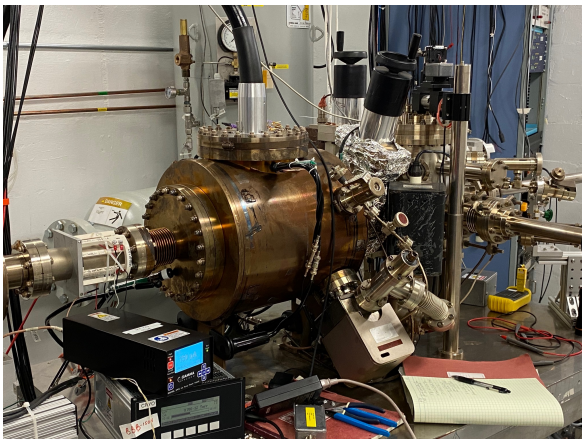

Fig. 9: Electron gun that produces the polarized electron beam.

3.1.2. *Wien filter*

The beam will go through a Wien filter, this device is built by using two plates of high voltage that produce an electric field, these are inside a vacuum chamber and around of them we have window coils that produce a magnetic field, so that we have

$$\vec{E} \perp \vec{B} \perp \vec{v}$$

and the equilibrium condition is accomplished when

$$e(\vec{E} + \vec{v} \times \vec{B} = 0).$$

This whole configuration is collocated inside a magnetic shell and once everything is mounted it looks like Fig. 10.

The function of the Wien filter is to rotate the direction of the spin by using the electric and magnetic fields, this effect is governed by the Thomas BMT equation [4], which leads us to

$$\theta = \frac{eL}{m_0 c\beta\gamma^2} B_x \tag{7}$$

Where θ is the angle that the spin is rotated.

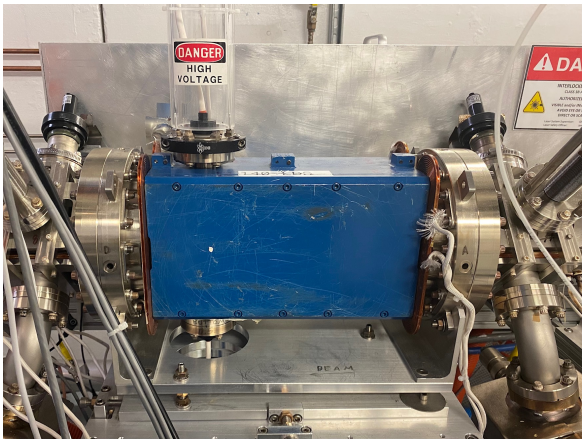

Fig. 10: Wien filter used in the beamline after being mounted.

3.2. Mott polarimeter

Once the electron beam enters the vacuum chamber of the Mott polarimeter it hits one of the golden foils, the electrons may be scattered and arrive to the detectors at 120°, data is taken and organized for its analyses.

3.3. Assymetry for one foil

For each one of the foils it is obtained how the energy changes over time by using the data acquisition system, as it is described on the section 2.2 (plots for CH1, CH2).
In the Fig. 11 the behavior for the target of 60 nm thickness of the left and right detectors at 120° can be seen, each function represents an electron. The behavior for 10 electrons is plotted.

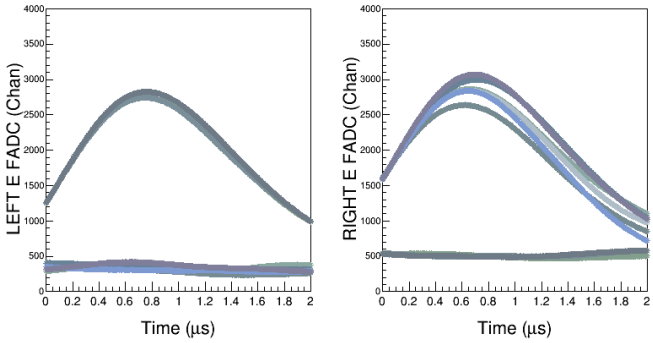

Fig. 11: Energy of each electron over time for the target of 60 nm thickness. The left and right plots represent the left and right detectors respectively.

In both graphics of the Fig. 11 there is a pedestal region which indicates that the electron did no hit that particular detector, for instance, when an electron is on the pedestal of the right detector its pulse is on the left detector, i.e. it hit the left detector but the right detector saw its reflection.

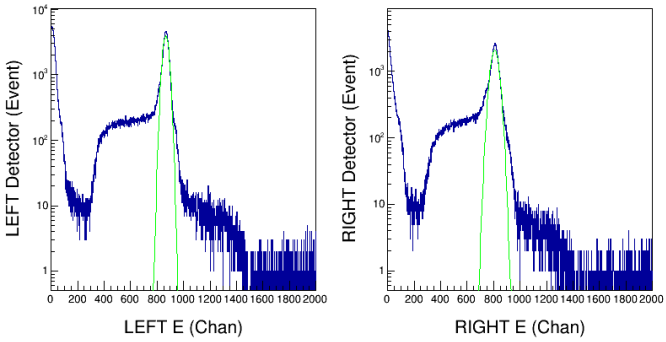

Fig. 12: Number of electrons with a certain energy for the target of 60 nm thickness. The left and right plots represent the left and right detectors respectively and the green plot is a Gaussian fit.

As its described on the section 2.2.1, to organize the data we can sum over the energies of the Fig. 11 and organize the data to obtain the histograms for the left and right detectors (see Fig. 12), or to obtain histograms with electrons of positive (red plot) and negative helicity (black plot), see Fig. 13, where, as we can see, the histogram for negative helicity is bigger in the left detector and in the right detector the histogram with positive helicity is bigger, this means that certain type of electrons hit one detector more than the other.

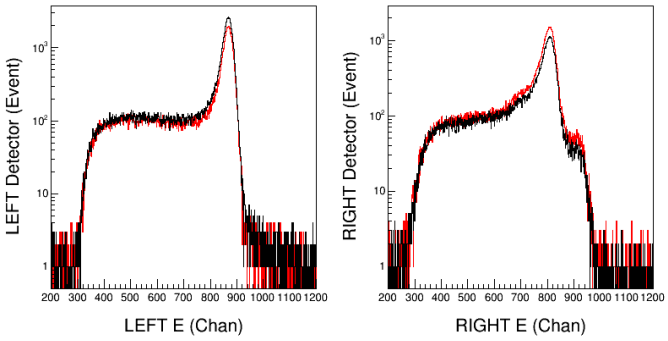

Fig. 13: Number of electrons with positive (red plot) and negative helicity (black plot) with a certain energy for the target of 60 nm thickness. The left and right plots represent the left and right detectors respectively.

These histograms represent the energy VS the number of electrons detected. For all the target foils the behaviors are similar to the ones showed in Fig. 11, 12 and 13.
In both histograms (Fig. 12 and 13) is necessary to perform a Gaussian fit, in Fig. 12 this can be seen in the green plot, we are interested in the portion that has higher number of electrons, the electrons near this region (between -0.5σ and 2σ) are the ones used to measure the asymmetry.

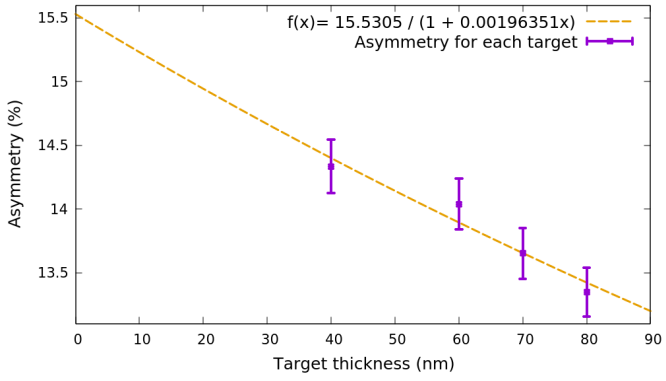

Fig. 14: Target thickness scan of the four target foils (black points) with their margin of error (blue lines) and fit (orange dashed function).

Given results of asymmetry for each target foil, a plot can be made as the Fig. 14 shows, where the target thickness

scan for the four golden foils is obtained. It can be seen that as the thickness of the target decreases the asymmetry factor increases.

A fit for these data is performed by using the function:

$$f(x) = \frac{a}{1+bx} \tag{8}$$

which leads to the following values of parameters for the data set:

$$a = 15.5305$$
$$b = 0.00196351$$

3.4. Obtaining the polarization

Due to the fitting of the data, it can be seen that when the target thickness approaches zero the asymmetry will take the value of a. By using equation (3) when the thickness is zero ($\epsilon_0 = PS_0$) and obtaining analytically the value of the Sherman functions for a 180 KV beam energy ($S_0 = -0.426135$) the polarization is obtained

$$\boxed{P = \frac{a}{S_0} = 36.45\%} \tag{9}$$

3.5. Asymmetry and current applied to the solenoids

The beamline contains two solenoids with fields A and B for focusing and directing the electron beam. It is interesting to notice how the asymmetry gets modified by varying the current applied to solenoids.

For the 40 nm thickness target foil we have the behavior that is shown in Fig. 15, where a sinusoidal fit was performed:

$$f(x) = a\sin(bx + c) \tag{10}$$

And the parameters have the following values:

$$a = 14.5858\ \%$$
$$b = 0.00367245 \text{ rad / } \Sigma \text{ of the fields}$$
$$c = -0.719592 \text{ rad}$$

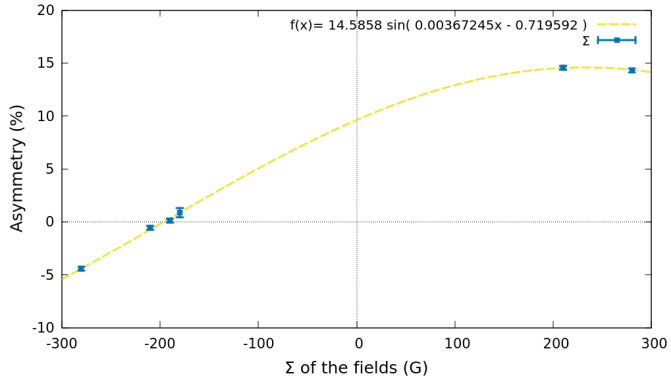

Fig. 15: Change of asymmetry as the factor (A - B) of the fields in the solenoids change for the target foil of 40 nm thickness. The fit can be seen with the yellow dashed line.

3.6. Asymmetry and voltage applied to Wien filter

On the other hand it is also important to show how the asymmetry factor gets modified as the voltage applied to the Wien filter increases, to illustrate this, the following plot is made for the target foil of 40 nm thickness, where another sinusoidal fit was performed just like the one used in the equation (10), however the values of the parameters change as it follows:

$$a = 14.2421\ \%$$
$$b = 0.0631088 \text{ rad / } \Sigma \text{ of the fields}$$
$$c = -0.153606 \text{ rad}$$

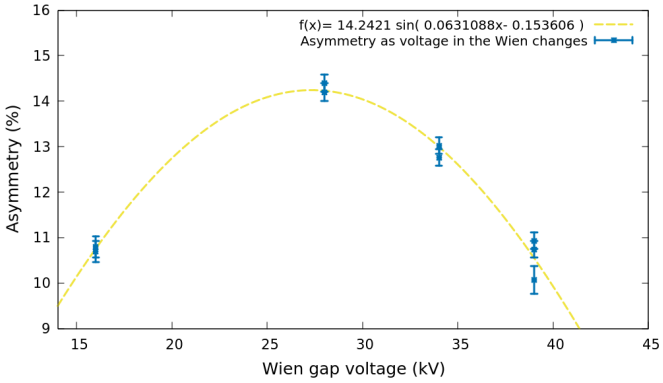

Fig. 16: Change of asymmetry as the voltage applied to the Wien filter is modified. The correspondent fit can be seen with the yellow dashed line.

4. CONCLUSIONS

- As can be seen, it is important to filter the data, to know which electrons we will use to make the final measurement.
- Once the electrons have been scattered, depending on their helicity, the detectors will find more electrons of one type than another, as shown in Fig. 13
- Thicker foils lead to smaller values of asymmetry since they contain more atoms and the electrons get scattered multiple times, i.e. the number of electrons that are detected in the left and right detector will be similar.
- By measuring the asymmetries for the four target foils and making a fit to the data set, it was able to find the value of asymmetry when the target thickness is zero. It is necessary to have enough data for an accurate fit.
- The polarization reached a value of $\sim 36\%$ which is congruent with other values found in the literature for an electron gun of this type with a GaAs photocatode.
- The asymmetry value gets modified when changing the solenoids current and the voltage of the Wien filter, in

both cases this change can be modeled with a sine function.

5. REFERENCES

[1] Grames, J. (2000). Measurement of a weak polarization sensitivity to the beam orbit of the CEBAF accelerator. *[Doctoral dissertation, University of Illinois at Urbana-Champaign]*.

[2] Gay, T. J., & Dunning, F. B. (1992). Mott electron polarimetry. *Review of Scientific Instruments*, 63(2), 1635–1651. https://doi.org/10.1063/1.1143371

[3] Barday, R., Aulenbacher, K., Bangert, P., Enders, J., Göök, A., Jakubassa-Amundsen, D. H., Nillius, F., Surzhykov, A., & Yerokhin, V. A. (2011). Compton transmission polarimeter for a very precise polarization measurement within a wide range of electron currents. *Journal of Physics: Conference Series*, 298, 012022. https://doi.org/10.1088/1742-6596/298/1/012022

[4] Fukuyama, T., & Silenko, A. J. (2013). Derivation of generalized Thomas-Bargmann-Michel-Telegdi equation for a particle with electric dipole moment. *International Journal of Modern Physics A*, 28(29), 1350147. https://doi.org/10.1142/s0217751x13501479